JOURNAL OF RESEARCH of the National Bureau of Standards — A. Physics and Chemistry
Vol. 70A, No. 6, November–December 1966

Viscoelastic Behavior Under Large Deformations

Louis J. Zapas

Institute for Basic Standards, National Bureau of Standards, Washington, D.C. 20234

(June 7, 1966)

The BKZ elastic fluid theory is used to correlate experimental results obtained in biaxial strain and steady simple shear. With a heuristic potential function involving three material properties, excellent agreement is obtained between theory and experiment. In the special case where one of the material properties is dominant, the behavior in steady simple shear is calculated from dynamic measurements in the infinitesimal range and is compared with actual data.

Key Words: BKZ theory, constant rate of strain, creep, elastic fluid, nonlinear behavior, polyisobutylene, recovery, stress, relaxation.

1. Introduction

In a recent paper [1],[1] excellent agreement was shown between experimental results and predictions of the BKZ elastic fluid theory [2]. This theory involves a potential function, U, but leaves it unspecified. For a given material, a knowledge of the results of a sufficient number of biaxial stress-relaxation experiments will enable one to predict with the BKZ theory the stress response to any other deformation history. However, if one knew a specific functional form by which U could be closely represented, then one would be able to correlate the behavior of different materials and different strain histories from the results of only a few experiments.

Encouraged by these results [1], I constructed a form of U with which the BKZ elastic fluid theory could quantitatively describe biaxial strain at large deformation, biaxial creep, and simple extension of vulcanized rubbers. This form of U involves three material properties. In simple shear it can quantitatively predict non-Newtonian behavior, including normal stresses. The ratio of the shearing stress to the rate of shear depends on the rate of shear in such a way as to describe either shear thinning or shear thickening behavior or both, depending on the relative magnitude of the material properties. In the special case where one material property is dominant, one may use dynamic data taken at infinitesimal strains to predict the dependence of viscosity and normal stresses on rate of shear. This is presented in section 4 of this paper and the agreement is excellent.

I want to emphasize that the form of U presented here is heuristic. The purpose of this paper is to show that with a relatively simple form of U, one may use the BKZ elastic fluid to describe very well the behavior of materials which can be considered isotropic and incompressible.

2. Theoretical Considerations

The BKZ elastic fluid is a fluid with an elastic potential. The effect of the configuration at time $\tau < t$ on the stress at time t is equivalent to the effect of a stored elastic energy with the configuration at time τ as the preferred configuration. The effect depends on the amount of time elapsed between τ and t. The stress at time t is the sum of contributions from all past times. For an extensive description of the theory, we refer the reader to the initial papers [2] and [3].

A particular motion of the material may be specified in terms of the Cartesian coordinates x_i of each particle at each time. Let X_1, X_2, X_3 be the position coordinates of the particles in a reference configuration. Then, a motion is given by a set of functions

$$x_i = x_i(X_k, t) \qquad i, k = 1, 2, 3. \tag{2.1}$$

At time τ, (2.1) becomes

$$x_i = x_i(X_k, \tau) \qquad i, k = 1, 2, 3. \tag{2.2}$$

If we eliminate X_1, X_2, X_3 between (2.1) and (2.2) we may write

$$x_i(t) = x_i(x_k(\tau), t, \tau) \qquad i, k = 1, 2, 3$$

where $x_i(t)$ and $x_i(\tau)$ are the position coordinates at time t and τ respectively of the same particle. The relative deformation gradients $x_{ik}(t, \tau)$ are defined by

$$x_{ik}(t, \tau) \equiv \frac{\partial x_i(t)}{\partial x_k(\tau)}.$$

The left Cauchy-Green tensor $c_{ij}(t, \tau)$ is then

$$c_{ij}(t, \tau) \equiv x_{ik}(t, \tau) x_{jk}(t, \tau)$$

[1] Figures in brackets indicate the literature references at the end of this paper.

where repeated indices indicate summation over the values 1, 2, 3.

The principal invariants of $c_{ij}(t, \tau)$ are

$$I_1(t, \tau) \equiv \zeta_1^2 + \zeta_2^2 + \zeta_3^2$$

$$I_2(t, \tau) \equiv \zeta_1^2\zeta_2^2 + \zeta_2^2\zeta_3^2 + \zeta_3^2\zeta_1^2$$

$$I_3(t, \tau) \equiv \zeta_1^2\zeta_2^2\zeta_3^2$$

where $\zeta_i^2 = \lambda_i^2(t, \tau)$ are the principal values of $c_{ij}(t, \tau)$ and λ_i is the stretch ratio in the x_i direction.

Assuming incompressibility, we have $I_3(t, \tau) = 1$, and the constitutive equations for the BKZ elastic fluid become [4]

$$\sigma_{ij}(t) = -p\delta_{ij} + 2\int_{-\infty}^{t}\left[\frac{\partial U}{\partial I_1}\, c_{ij}(t, \tau) - \frac{\partial U}{\partial I_2}\, c_{ij}^{-1}(t, \tau)\right] d\tau \quad (2.3)$$

where σ_{ij} are the components of the stress tensor, p is a hydrostatic pressure, U is a function of I_1, I_2, and $t-\tau$

$$U = U(I_1(t, \tau), I_2(t, \tau), t-\tau),$$

and $c_{ij}^{-1}(t, \tau)$ are the components of the inverse of the matrix $\|c_{ij}(t, \tau)\|$. We may describe an isochoric homogeneous biaxial strain history by writing for (2.1)

$$x_1(t) = \lambda_1(t)X_1$$

$$x_2(t) = \lambda_2(t)X_2$$

$$x_3(t) = \lambda_3(t)X_3 = \frac{1}{\lambda_1\lambda_2}X_3.$$

The matrix of the left Cauchy-Green tensor $c_{ij}(t, \tau)$ becomes

$$\|c_{ij}(t, \tau)\| = \begin{Vmatrix} \dfrac{\lambda_1^2(t)}{\lambda_1^2(\tau)} & 0 & 0 \\ 0 & \dfrac{\lambda_2^2(t)}{\lambda_2^2(\tau)} & 0 \\ 0 & 0 & \dfrac{\lambda_1^2(\tau)\lambda_2^2(\tau)}{\lambda_1^2(t)\lambda_2^2(t)} \end{Vmatrix}$$

and

$$I_1(t, \tau) = \frac{\lambda_1^2(t)}{\lambda_1^2(\tau)} + \frac{\lambda_2^2(t)}{\lambda_2^2(\tau)} + \frac{\lambda_1^2(\tau)\lambda_2^2(\tau)}{\lambda_1^2(t)\lambda_2^2(t)} \quad (2.4)$$

$$I_2(t, \tau) = \frac{\lambda_1^2(\tau)}{\lambda_1^2(t)} + \frac{\lambda_2^2(\tau)}{\lambda_2^2(t)} + \frac{\lambda_1^2(t)\lambda_2^2(t)}{\lambda_1^2(\tau)\lambda_2^2(\tau)}. \quad (2.5)$$

From (2.3), (2.4), and (2.5) we get

$$\sigma_{11}(t) - \sigma_{33}(t) = 2\int_{-\infty}^{t}\left[\frac{\lambda_1^2(t)}{\lambda_1^2(\tau)} - \frac{\lambda_1^2(\tau)\lambda_2^2(\tau)}{\lambda_1^2(t)\lambda_2^2(t)}\right]\left[\frac{\partial U}{\partial I_1} + \frac{\lambda_2^2(t)}{\lambda_2^2(\tau)}\frac{\partial U}{\partial I_2}\right] d\tau \quad (2.6)$$

and

$$\sigma_{22}(t) - \sigma_{33}(t) = 2\int_{-\infty}^{t}\left[\frac{\lambda_2^2(t)}{\lambda_2^2(\tau)} - \frac{\lambda_1^2(\tau)\lambda_2^2(\tau)}{\lambda_1^2(t)\lambda_2^2(t)}\right]\left[\frac{\partial U}{\partial I_1} + \frac{\lambda_1^2(t)}{\lambda_1^2(\tau)}\frac{\partial U}{\partial I_2}\right] d\tau. \quad (2.7)$$

In the case of a single step stress-relaxation experiment where $\lambda_i(\tau) = 1$ for times τ smaller than zero and $\lambda_i(\tau) = \lambda_i(t) = \lambda_i$ for times t, τ greater than zero, (2.6) yields

$$\frac{\sigma_{11}(t) - \sigma_{33}(t)}{\lambda_1^2 - \dfrac{1}{\lambda_1^2\lambda_2^2}} = 2\left(\frac{\partial W}{\partial I_1} + \lambda_2^2\frac{\partial W}{\partial I_2}\right) \quad (2.8)$$

where

$$W = W(I_1, I_2, t) \equiv \int_t^{\infty} U(I_1, I_2, \xi)d\xi, \quad (2.9)$$

$$\xi = t - \tau,$$

and

$$I_1 = \lambda_1^2 + \lambda_2^2 + \frac{1}{\lambda_1^2\lambda_2^2}$$

$$I_2 = \frac{1}{\lambda_1^2} + \frac{1}{\lambda_2^2} + \lambda_1^2\lambda_2^2$$

Similarly (2.5) becomes

$$\frac{\sigma_{22}(t) - \sigma_{33}(t)}{\lambda_2^2 - \dfrac{1}{\lambda_1^2\lambda_2^2}} = 2\left(\frac{\partial W}{\partial I_1} + \lambda_1^2\frac{\partial W}{\partial I_2}\right) \quad (2.10)$$

Superficially, expressions (2.8) and (2.10) appear to be the same as the relations given by Rivlin and Saunders [5]. However W, here, depends on time as well as strain and is designed so that (2.10) gives the stress during stress relaxation. On the other hand, the W of Rivlin and Saunders depends only on strain.

In the case of simple shear, we introduce an orthogonal set of coordinates as shown in figure 1, where x_1 is the direction of motion of a particle and x_2 is the direction of shear. In the case of a steady shearing

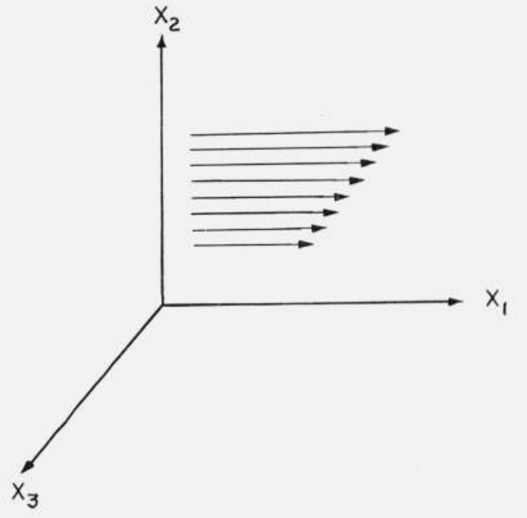

FIGURE 1. *General coordinate axes for description of flow.*

motion with constant rate of shear, $\dot{\gamma}$, (2.1) reads

$$x_1(t)=x_1(\tau)+(t-\tau)\dot{\gamma}x_2(\tau)$$

$$x_2(t)=x_2(\tau)$$

$$x_3(t)=x_3(\tau)$$

Thus,

$$\| c_{ij}(t,\tau)\| = \begin{Vmatrix} 1+\dot{\gamma}^2(t-\tau)^2 & \dot{\gamma}(t-\tau) & 0 \\ \dot{\gamma}(t-\tau) & 1 & 0 \\ 0 & 0 & 1 \end{Vmatrix}$$

and

$$\| c_{ij}^{-1}(t,\tau)\| = \begin{Vmatrix} 1 & -\dot{\gamma}(t-\tau) & 0 \\ -\dot{\gamma}(t-\tau) & 1+\dot{\gamma}^2(t-\tau)^2 & 0 \\ 0 & 0 & 1 \end{Vmatrix}$$

Substituting in equation (2.3) with $t-\tau=\xi$, one gets

$$\sigma_{12}=2\int_0^\infty \left\{\frac{\partial U}{\partial I_1}+\frac{\partial U}{\partial I_2}\right\}\dot{\gamma}\xi d\xi \qquad (2.11)$$

where

$$I_1(t,t-\xi)=I_2(t,t-\xi)=3+\dot{\gamma}^2\xi^2$$

and

$$U=U(I_1,I_2,\xi)$$

$$\sigma_{11}=-p+2\int_0^\infty \left\{\frac{\partial U}{\partial I_1}(1+\dot{\gamma}^2\xi^2)-\frac{\partial U}{\partial I_2}\right\}d\xi \qquad (2.12)$$

$$\sigma_{22}=-p+2\int_0^\infty \left\{\frac{\partial U}{\partial I_1}-\frac{\partial U}{\partial I_2}(1+\dot{\gamma}^2\xi^2)\right\}d\xi \qquad (2.13)$$

$$\sigma_{33}=-p+2\int_0^\infty \left\{\frac{\partial U}{\partial I_1}-\frac{\partial U}{\partial I_2}\right\}d\xi. \qquad (2.14)$$

These relations hold independently of the form of U.

3. Experimental Procedure

From the theoretical considerations of the previous section, we see that we may determine $\partial W/\partial I_1$ and $\partial W/\partial I_2$ as functions of I_1, I_2, and t from data taken in single step stress-relaxation experiments in biaxial strain. For vulcanized rubbers we may regard the long time isochrones in creep to within a good approximation as isochrones of single step stress relaxation. This is true for a material only if the deformation at constant load remains almost constant for long times, although not necessarily to infinite time. For this reason we elected to do our experiments on vulcanized butyl rubber. The experiments were carried out using a test piece in the form of a square sheet having sides of 8 cm and a thickness of about 0.07 cm. The test piece was cut and marked in a fashion described by Rivlin and Saunders [5]. One square surface of the sheet was marked in ink with two sets of four parallel straight lines so as to form a square grid with 1 cm spacings. In drawing the outer lines of the grid, great care was taken that they be straight and form a *perfect* square. In figure 2 is shown part of the ap-

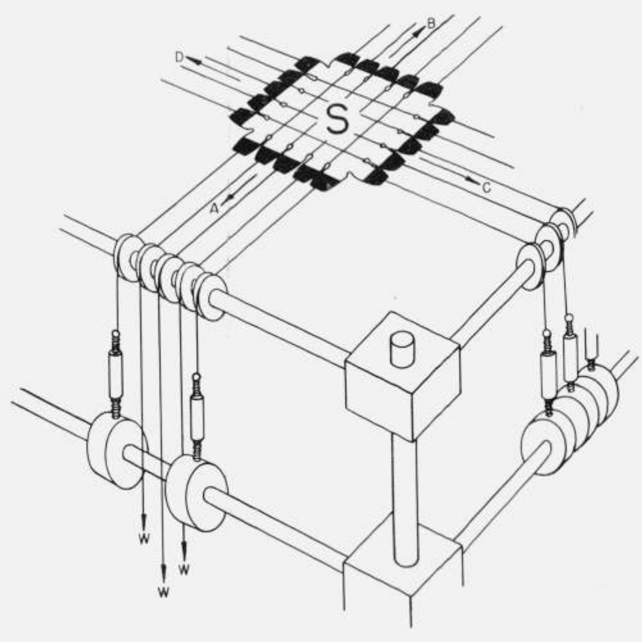

FIGURE 2. *Schematic diagram for the biaxial extension experiments.*

paratus with the sample S. As can be seen from the figure, the sample was stretched in the A–B and C–D directions with the aid of strings. One end of each string was tied to a lug of the sample and the other end was attached to a weight or to a turnbuckle. The strings were made from unspun fibers of Mylar. For the study of the variation of $\partial W/\partial I_1$ and $\partial W/\partial I_2$ with respect to time, the two sets of the three middle lugs in the A and C directions were tied to strings supporting weights. The other 14 lugs were tied to strings in which tension was controlled with the turnbuckles, which could be adjusted to keep the ink lines on the sample straight and parallel. With the aid of a two-way traveling microscope, whose axes of travel were set parallel to the stretch directions, we could check the uniformity of stretch and measure the extensions.

In our other sets of biaxial experiments, we loaded the sample by first stretching it a predetermined amount in the D–C direction and then applying weights in the A–B direction. This was done in order to avoid difficulties due to the history of loading. In these experiments, only the three middle lugs in the A direction carried supporting weights. The strings attached to the other lugs were adjusted to keep the lines straight and parallel to the stretch directions. The final readings were taken after 18 hr from the time of loading. After each measurement the material was allowed to relax for 24 to 48 hr before another loading was started. Thus, the values that we obtained can be considered as isochronal values of stress relaxation at 18 hr.

In order to be able to compare with experiment the predictions of our theory for simple shear flows, we performed dynamic and constant rate of shear measurements on solutions of polyisobutylene B–140 in Mentor 28 oil. Two concentrations were used. They shall be designated as 10 percent and 5 percent. We do not know the actual concentration accurately, because we lost an unknown amount of solvent while preparing what was to be the 10 percent solution. We do know that the ratio of the two concentrations is two to one. The dynamic data at very small deformations were obtained through the cooperation of R. W. Penn, using a torsion pendulum at the W. R. Grace Laboratories. The torsion pendulum is essentially the same as the one described by Morrison, Zapas, and DeWitt [6]. The data on viscosity as a function of rate of shear were obtained in a capillary viscometer.

4. Experimental Results and Discussion

The purpose of this paper is to show that with a relatively simple form of the potential function U, the BKZ elastic fluid can be used to correlate different types of behavior of elastomeric materials. The heuristic form of the potential function U which I shall use here involves three material properties $\alpha(t)$, $\beta(t)$, and $c(t)$. These material properties are positive monotonically decreasing functions of time. The form of U is given by the following expression:

$$-U=\frac{\alpha'}{2}(I_1-3)^2+4.5\beta' \ln\left(\frac{I_1+I_2+3}{9}\right)+24(\beta'-c')\ln\left(\frac{I_1+15}{I_2+15}\right)+c'(I_1-3) \qquad (4.1)$$

where

$$\alpha'=\frac{d\alpha(t)}{dt},\ \beta'=\frac{d\beta(t)}{dt},\ \text{and } c'=\frac{dc(t)}{dt}.$$

From equations (2.9) and (4.1) we get

$$\frac{\partial W}{\partial I_1}=\alpha(I_1-3)+\frac{4.5\beta}{I_1+I_2+3}+\frac{24(\beta-c)}{I_1+15}+c \qquad (4.2)$$

$$\frac{\partial W}{\partial I_2}=\frac{4.5\beta}{I_1+I_2+3}-\frac{24(\beta-c)}{I_2+15} \qquad (4.3)$$

where it is understood W, α, β, and c are functions of time.

In a pure shear single step stress-relaxation experiment with $\lambda_2=1$, and $I_1=I_2$, we get from eq (2.8)

$$\frac{\sigma_{11}(t)-\sigma_{33}(t)}{\lambda_1^2-\frac{1}{\lambda_1^2}}=2\left(\frac{\partial W}{\partial I_1}+\frac{\partial W}{\partial I_2}\right)$$

$$=2\left\{\alpha(I_1-3)+\frac{9\beta}{2I_1+3}+c\right\} \qquad (4.4)$$

Since $\alpha(t)$ is taken to be a positive monotonically decreasing function of time, or zero, eq (4.4) says that if one plots $\frac{\sigma_{11}(t)-\sigma_{33}(t)}{\lambda_1^2-\frac{1}{\lambda_1^2}}$ at constant t versus $\frac{1}{2I_1+3}$, one should get either a curve which is concave upward or a straight line. In the case of a straight line the slope is equal to 18β, the intercept, $2c$, and α equals zero.

In figure 3 we show the data of Rivlin and Saunders [5] on pure shear for vulcanized natural rubber. In this figure we plotted $\frac{\sigma_{11}-\sigma_{33}}{2\left(\lambda_1^2-\frac{1}{\lambda_1^2}\right)}-\alpha(I_1-3)$ versus $\frac{1}{2I_1+3}$ for $\alpha=0$ and $\alpha=0.06$. As can be seen for the case where $\alpha=0$, the curve is concave upwards. Here $\alpha=0.06$ was found by trial and error. Actually, if there is a well defined minimum, one could obtain α by following the procedure presented in a previous paper [3]. So it is evident that by using the relation (4.4) one could get the three material properties from pure shear experiments.

In figure 4 we present a similar check of the adequacy of the assumed form of U by plotting

$$\frac{\sigma_{11}(t)-\sigma_{33}(t)}{2\left(\lambda_1^2-\frac{1}{\lambda_1^2\lambda_2^2}\right)}-\alpha(I_1-3)\ \text{versus}\ \frac{1+\lambda_2^2}{I_1+I_2+3}$$

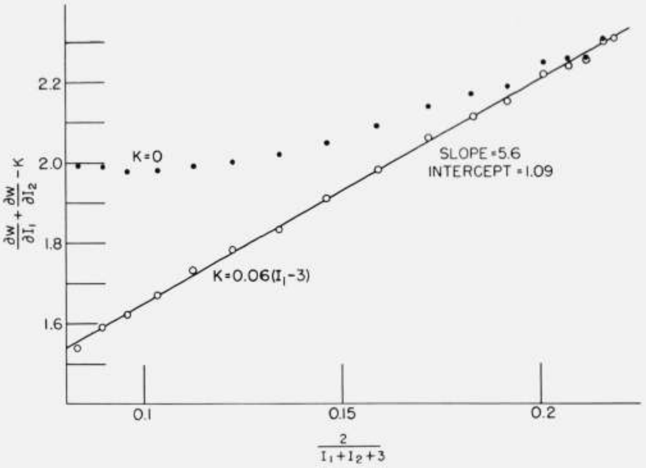

FIGURE 3. *Pure shear data of Rivlin and Saunders on vulcanized natural rubber.*
Open circles, $\alpha=0$. The abscissa is given in kg per cm².

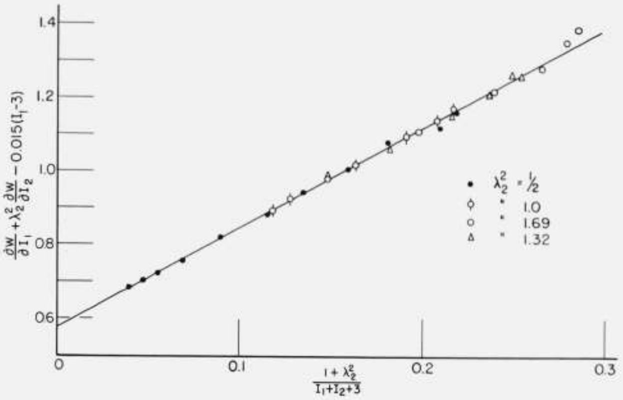

FIGURE 4. *Biaxial extension data of vulcanized butyl rubber.*
The abscissa is given in (dynes/cm²)10^{-6}.

using data obtained on vulcanized butyl rubber in biaxial and simple extension deformations as described in the previous section. For butyl rubber, the value of $\alpha(t)$ is small and estimated to be 0.015. Since β and c are equal, as determined from the pure shear data, in a plot of this type the experimental points should fall in a straight line. Considering experimental difficulties and uncertainties, the agreement is excellent.

TABLE 1. *Biaxial creep of vulcanized butyl rubber*

Time	I_1	I_2	$\frac{\partial W}{\partial I_1}\times 10^{-6}$	$\frac{\partial W}{\partial I_2}\times 10^{-6}$
Hours			*Dynes/cm²*	*Dynes/cm²*
3	3.1043	3.1050	2.15	−0.10
20	3.1125	3.1125	1.91	.07
23	3.1134	3.1131	1.83	.14
47	3.1160	3.1156	1.80	.16
66	3.1177	3.1172	1.78	.17
90	3.1199	3.1191	1.74	.19
117	3.1211	3.1203	1.71	.20
164	3.1233	3.1224	1.69	.21

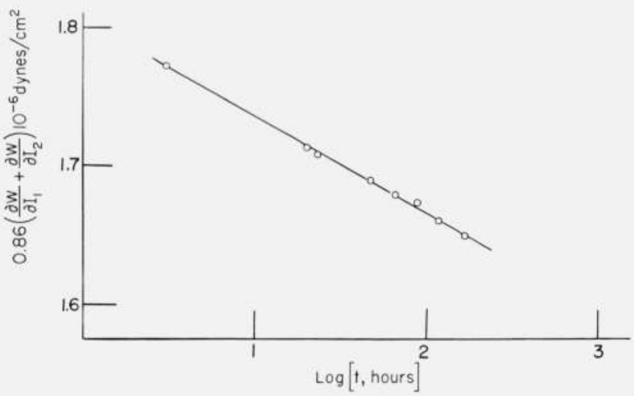

FIGURE 5. *Biaxial creep data on vulcanized butyl rubber.*

In the course of our experiments in biaxial deformation, in a different set of measurements we observed a negative value of $\partial W/\partial I_2$ at very small extensions, while at higher extensions $\partial W/\partial I_2$ was positive. This was observed in three samples with different degrees of vulcanization. For a further study of this peculiarity we selected a relatively high cross-linked specimen of butyl rubber and we studied its biaxial creep behavior at small deformations. In table 1 we show the calculated values of $\partial W/\partial I_1$ and $\partial W/\partial I_2$ as functions of I_1, I_2, and time. This table shows large variations in $\partial W/\partial I_2$ for small changes in I_1 and I_2. A plot of $\partial W/\partial I_1+\partial W/\partial I_2$ versus the logarithm of time is shown in figure 5. We see that even in greatly expanded scale for $\partial W/\partial I_1+\partial W/\partial I_2$ the points fall in a straight line. Moreover, after 150 hr the data still did not indicate any suggestions of leveling off. This shows that we cannot neglect the behavior with respect to time. From single step stress-relaxation experiments in simple extension in vulvanized rubbers, we observed that β decays with time much faster than c. From (4.3) we can see that $\partial W/\partial I_2$ will be negative when β is larger than 1.6c. One can see, at least qualitatively, that what seemed to be a paradoxical inversion in sign for $\partial W/\partial I_2$ is predictable from eq (4.3).

4.1. Steady Simple Shearing Flow

We can substitute eq (4.1) into eq (2.11) to get

$$\sigma_{12}=-2\int_0^\infty\left\{\alpha'(\xi)\dot{\gamma}^2\xi^2+\frac{9\beta'(\xi)}{9+2\dot{\gamma}^2\xi^2}+c'(\xi)\right\}\dot{\gamma}\xi d\xi. \tag{4.5}$$

Since the viscosity $\eta(\dot{\gamma})$ is defined to be the ratio of σ_{12} to $\dot{\gamma}$, eq (4.5) can be written

$$\eta(\dot{\gamma})=-2\int_0^\infty \left\{\alpha'(\xi)\dot{\gamma}^2\xi^2+\frac{9\beta'(\xi)}{9+2\dot{\gamma}^2\xi^2}+c'(\xi)\right\}\xi d\xi. \tag{4.6}$$

By considering special cases for which the dominant term is that containing $\alpha'(\xi)$, $\beta'(\xi)$, or $c'(\xi)$, one can see that (4.6) could predict a viscosity independent of rate of shear, or viscosities as observed in shear thinning or shear thickening materials.

In figure 6 we show schematically the type of behavior predicted from eq (4.6). For the sake of simplicity we can write

$$\eta(\dot{\gamma})=\eta_\alpha(\dot{\gamma})+\eta_\beta(\dot{\gamma})+\eta_c \tag{4.7}$$

where

$$\eta_\alpha(\dot{\gamma})=-2\int_0^\infty \alpha'(\xi)\dot{\gamma}^2\xi^3 d\xi \tag{4.7a}$$

$$\eta_\beta(\dot{\gamma})=-2\int_0^\infty \frac{\beta'(\xi)\xi}{1+\frac{2}{9}\dot{\gamma}^2\xi^2}d\xi \tag{4.7b}$$

$$\eta_c=-2\int_0^\infty c'(\xi)\xi d\xi \tag{4.7c}$$

We observe that in the case where $\eta_\alpha(\dot{\gamma})=\eta_\beta(\dot{\gamma})=0$ one gets a viscosity independent of rate of shear. When only $\eta_\alpha(\dot{\gamma})=0$, one gets a behavior shown in curve II of figure 6. Curves III and IV represent the cases where $\eta_\alpha(\gamma)$, $\eta_\beta(\dot{\gamma})$, and η_c all contribute to the viscosity. Naturally, curve IV shows the case where $\eta_\alpha(\dot{\gamma})$ is the dominant quantity.

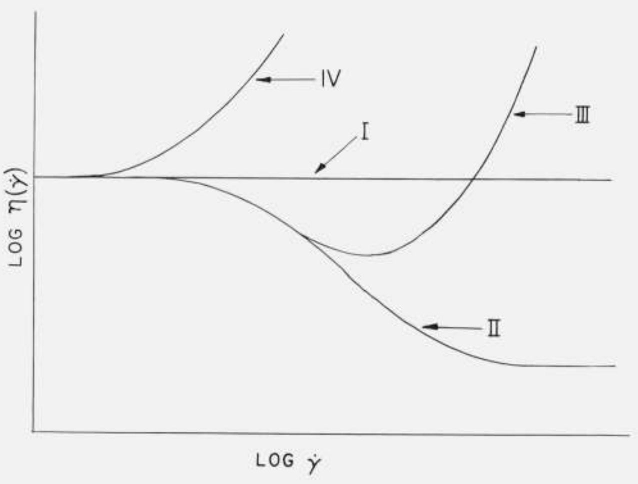

FIGURE 6. *Schematic representation of forms of steady shear viscosity curves which can be predicted by eq (4.6).*

4.2. Comparison of Steady Simple Shearing Flow With Measurements at Infinitesimal Deformations

For a simple shear deformation, which is specified in terms of a single parameter, say $\gamma=\gamma(\tau)$, (2.2) may be written

$$\begin{aligned} x_1(\tau)&=X_1+\gamma(\tau)X_2\\ x_2(\tau)&=X_2\\ x_3(\tau)&=X_3. \end{aligned} \tag{4.8}$$

To represent single step stress relaxation, we take $\gamma(\tau)=0$ for $\tau<0$ and $\gamma(\tau)=\gamma=$constant for $\tau>0$, and we get

$$\|c_{ij}\|=\begin{Vmatrix}1+\gamma^2 & \gamma & 0\\ \gamma & 1 & 0\\ 0 & 0 & 1\end{Vmatrix}$$
$$\|c_{ij}^{-1}\|=\begin{Vmatrix}1 & -\gamma & 0\\ -\gamma & 1+\gamma^2 & 0\\ 0 & 0 & 1\end{Vmatrix} \tag{4.9}$$

where $I_1=I_2=3+\gamma^2$. From (2.3), (2.9), (4.2), (4.3), and (4.9), we obtain

$$\sigma_{12}(t)=2\gamma\left[\gamma^2\alpha(t)+\frac{9\beta(t)}{9+2\gamma^2}+c(t)\right]. \tag{4.10}$$

The limit of $\frac{\sigma_{12}(t)}{\gamma}$ for vanishing γ gives us the relaxation function, $G(t)$, for infinitesimal deformations:

$$G(t)=2\beta(t)+2c(t). \tag{4.11}$$

From the general relation of linear viscoelasticity [7] between periodic and steady-state functions

$$G'(\omega)+i\omega\eta'(\omega)=i\omega\int_0^\infty G(t)e^{-i\omega t}dt,$$

we can express $\eta'(\omega)$ in terms of $\beta(t)$ and $c(t)$ as

$$\eta'(\omega)=\int_0^\infty \{2\beta(t)+2c(t)\}\cos\omega t dt. \tag{4.12}$$

Integrating (4.6) by parts we get

$$\eta(\dot{\gamma})=2\int_0^\infty \left\{3\alpha(\xi)\dot{\gamma}^2\xi^2+\frac{9\beta(\xi)(9-2\dot{\gamma}^2\xi^2)}{(9+2\dot{\gamma}^2\xi^2)^2}+c(\xi)\right\}d\xi \tag{4.13}$$

Several interesting observations can be drawn regarding the behavior of a material which can be described by a potential function U of the form of (4.1) by comparing (4.12) and (4.13). First, it is obvious that in general $\eta(\dot{\gamma})$ cannot be predicted from measurements of $\eta'(\omega)$, since the term in $\alpha(t)$ does not show up in $\eta'(\omega)$ at all. Also, $\beta(t)$ and $c(t)$ cannot be separated by measurements of $\eta'(\omega)$. However, if we encounter a material for which either β or c is the dominant term in (4.13) and (4.9) then in principle $\eta(\dot{\gamma})$ can be calculated from $\eta'(\omega)$. If c is the dominant term, we will have a situation in which $\eta(\dot{\gamma})$ is independent of rate of shear, but $\eta'(\omega)$ may vary with frequency and normal stress effects may be observed in steady shearing flow. If β is dominant, both $\eta'(\omega)$ and $\eta(\dot{\gamma})$ will vary with ω or $\dot{\gamma}$.

For many materials $\alpha(t)$ is negligible, but ordinarily both $\beta(t)$ and $c(t)$ contribute to $\eta(\dot{\gamma})$, with $\beta(t)$ contributing the dominant term within experimentally accessible rates of shear. However, at very high rates of shear, any nonzero c must become dominant. For the range of rates of shear for which

$$\int_0^\infty \frac{9\beta(\xi)(9-2\dot{\gamma}^2\xi^2)}{(9+2\dot{\gamma}^2\xi^2)^2}\,d\xi \gg \int_0^\infty c(\xi)d\xi$$

we may utilize $\eta'(\omega)$ to evaluate $\beta(t)$ and calculate a lower bound for the measured $\eta(\dot{\gamma})$. The calculated $\eta(\dot{\gamma})$ should be in close agreement with that measured at low values of $\dot{\gamma}$, but would fall below the measured values at high rates of shear.

For the actual comparison of the two measured functions $\eta'(\omega)$ and $\eta(\dot{\gamma})$, it is better to formulate our expressions in terms of relaxation spectra corresponding to $\beta(t)$ and $c(t)$ entirely analogous to the spectrum representation of $G(t)$. The relaxation spectrum $F(\tau)$ may be defined by [7]:

$$G(t)=\int_0^\infty F(\tau)e^{-t/\tau}d\tau$$

and may be expressed as the sum of two terms $F_\beta(\tau)$ and $F_c(\tau)$ defined by

$$2\beta(t)=\int_0^\infty F_\beta(\tau)e^{-t/\tau}d\tau$$
$$2c(t)=\int_0^\infty F_c(\tau)e^{-t/\tau}d\tau. \tag{4.14}$$

In terms of (4.14) we have

$$G'(\omega)=\int_0^\infty \frac{\{F_\beta(\tau)+F_c(\tau)\}\omega^2\tau^2d\tau}{1+\omega^2\tau^2} \tag{4.15}$$

$$\eta'(\omega)=\int_0^\infty \frac{\{F_\beta(\tau)+F_c(\tau)\}\tau d\tau}{1+\omega^2\tau^2} \tag{4.16}$$

and in the case where $\alpha(t)\equiv 0$ from eq (4.6)

$$\eta(\dot{\gamma})=\int_0^\infty \left\{F_\beta(\tau)\tau\int_0^\infty \frac{xe^{-x}dx}{1+\frac{2}{9}\dot{\gamma}^2\tau^2x^2}+\tau F_c(\tau)\right\}d\tau. \tag{4.17}$$

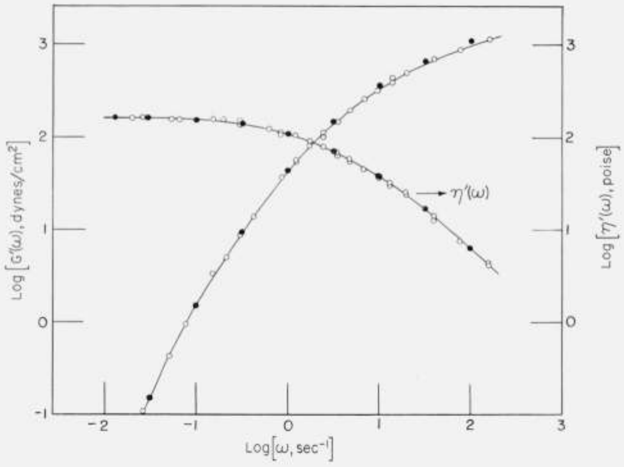

FIGURE 7. *Dynamic data on 5 percent solution of B−140 in Mentor 28 oil.* Solid circles represent the values calculated from data given in table 2.

TABLE 2. *Relaxation spectrum for 5 percent solution of polyisobutylene B−140 in Mentor 28 at 25 °C*

τ	$H(\tau)$
19.0	0.0
15.2	.1
10	.5
3	7.3
1.0	39
0.3	120
.1	245
.03	410
.01	420

We calculated $H(\tau)=\tau F(\tau)$ from measurements of $\eta'(\omega)$ and $G'(\omega)$ on the five percent solution of B−140 by an iterative method which will be described in another paper. In figure 7 we show the dynamic rigidity and viscosity as a function of frequency. The black points represent points calculated from $H(\tau)$ as obtained by our iterative method and tabulated in table 2. The agreement indicates that we have a good representation within the range of measurements. In figure 8 we show the viscosity at steady shearing flow as a function of rate of shear, with the open circles representing values calculated from eq (4.17) assuming that the contribution of the integral of $F_c(\tau)\tau$ is negligible. The agreement between experimental and calculated values is excellent.

The same arguments can be used for the determination of the normal stress differences $\sigma_{11}-\sigma$, $\sigma_{22}-\sigma$, and $\sigma_{33}-\sigma$ (where $3\sigma=\sigma_{11}+\sigma_{22}+\sigma_{33}$) as can be seen from eqs (2.12) to (2.14). An interesting result is that the limiting value of the ratio $\frac{\sigma_{22}-\sigma_{33}}{\sigma_{11}-\sigma_{33}}$ at small rates of shear is 0.46 in the case where β is the dominant term. This compares very well with the value of 0.4 reported by Markovitz [8] for a 5.39 percent solution of polyisobutylene in cetane.

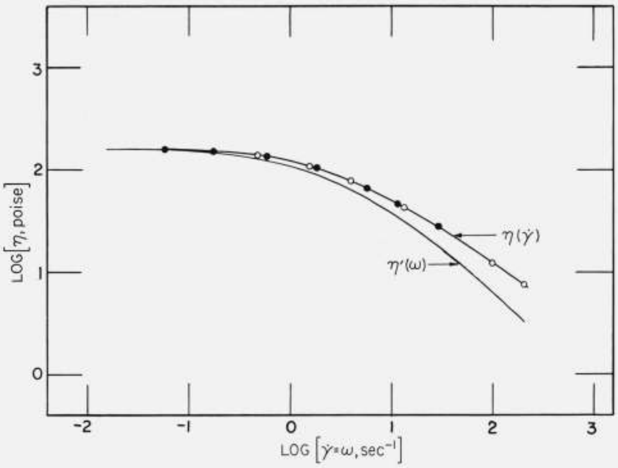

FIGURE 8. *Dynamic viscosity and steady shear viscosity data on 5 percent solution of B−140 in Mentor 28 oil.*

Solid circles are the calculated values.

In conclusion, we should emphasize that all these derivations were obtained with the assumption of incompressibility. In reality $\partial W/\partial I_1$ and $\partial W/\partial I_2$ depend also on I_3, the influence of which can not be evaluated from the experiments reported above.

I thank B. Bernstein, E. A. Kearsley, and R. S. Marvin for their valuable discussions during the preparation of this manuscript.

5. References

[1] L. J. Zapas and T. Craft, J. Res. NBS **69A** (Phys. and Chem.) No. 6, 541–546 (1965).

[2] B. Bernstein, E. A. Kearsley, and L. J. Zapas, J. Res. NBS **68B** (Math. and Math. Phys.) No. 4, 103–113 (1964).

[3] B. Bernstein, E. A. Kearsley, and L. J. Zapas, Trans. Soc. Rheology **VII**, 391–410 (1963).

[4] B. Bernstein, Time-dependent behavior of an imcompressible elastic fluid—Some homogeneous deformations, to be published in Acta Mechanica.

[5] R. S. Rivlin and D. W. Saunders, Phil. Trans, Roy. Soc. London, A **243**, 251 (1951).

[6] J. E. Morrisson, L. J. Zapas, and J. W. DeWitt, Rev. Sci. Instr. **26**, 357 (1955).

[7] J. D. Ferry, Viscoelastic Properties of Polymers, (John Wiley & Sons, New York and London, 1961).

[8] H. Markovitz, Proceedings of the Fourth International Congress on Rheology, Part I, 189 (1963).

(Paper 70A6–423)